4002 J. Med. Chem. 2010, 53, 4002–4008
DOI: 10.1021/jm901853b

Journal of Medicinal Chemistry Article

Structural Evidence That Human Acetylcholinesterase Inhibited by Tabun Ages through O-Dealkylation†

Eugénie Carletti,‡,§ Jacques-Philippe Colletier,‡ Florine Dupeux,∥ Marie Trovaslet,§ Patrick Masson,‡,§ and Florian Nachon*,§

‡Laboratoire de Biophysique Moléculaire, Institut de Biologie Structurale (CEA-CNRS-UJF), 41 rue Jules Horowitz, 38027 Grenoble, France, §Département de Toxicologie, Centre de Recherches du Service de Santé des Armées (CRSSA), 24 av des Maquis du Grésivaudan, 38700 La Tronche, France, and ∥European Molecular Biology Laboratory, Grenoble Outstation Polygon Scientific, 6 rue Jules Horowitz, 38000 Grenoble, France

Received December 15, 2009

Tabun is a warfare agent that inhibits human acetylcholinesterase (hAChE) by rapid phosphylation of the catalytic serine. A time-dependent reaction occurs on the tabun adduct, leading to an "aged" enzyme, resistant to oxime reactivators. The aging reaction may proceed via either dealkylation or deamidation, depending on the stereochemistry of the phosphoramidyl adduct. We solved the X-ray structure of aged tabun−hAChE complexed with fasciculin II, and we show that aging proceeds through O-dealkylation, in agreement with the aging mechanism that we determined for tabun-inhibited human butyrylcholinesterase and mouse acetylcholinesterase. Noteworthy, aging and binding of fasciculin II lead to an improved thermostability, resulting from additional stabilizing interactions between the two subdomains that face each other across the active site gorge. This first structure of hAChE inhibited by a nerve agent provides structural insight into the inhibition and aging mechanisms and a structural template for the design of molecules capable of reactivating aged hAChE.

Introduction

Acetylcholinesterase (AChE;[a] EC 3.1.1.7) is the target of numerous natural and synthetic inhibitors, for example, fasciculin, a polypeptide neurotoxin found in mamba snake venom;[1] therapeutic drugs, in particular the first generation of anti-Alzheimer drugs;[2] and a wide range of toxic esters, including organophosphate (OP) pesticides and nerve agents.[3] AChE regulates cholinergic transmission in the peripheral and central nervous systems by hydrolyzing acetylcholine (ACh) with a high catalytic efficiency. Although butyrylcholinesterase (BChE; EC 3.1.1.8), a closely related enzyme, is present in numerous vertebrate tissues, its physiological role remains unclear.[4] While BChE inhibition appears harmless, AChE inhibition results in accumulation of ACh at neuronal synapses and neuromuscular junctions and results in paralysis, seizures, and other symptoms of cholinergic syndrome.[5,6]

The AChE catalytic site, featuring a Ser203−His447−Glu334 triad [residue numbering refers to human AChE (hAChE) throughout the manuscript, unless stated otherwise], is at the bottom of a deep and narrow gorge[7] (Figure 1). AChE inhibition can result from binding either to the gorge entrance, called the "peripheral anionic site" (PAS) (viz. fasciculin), or to the active site (viz. OP). Inhibition of human AChE by OP compounds involves phosphylation of the catalytic serine and leads to the formation of stable inactive phosphyl−AChE adducts. Within the active site, substantial contributions to the stabilization of bound OP within the active site arises from hydrogen bonding of the phosphyl oxygen within the oxyanion hole, viz. Gly121, Gly122, and Ala204, and one of its substituents in the "acyl pocket", viz. Trp236, Phe295, Phe297, and Phe338. Reaction of OP−hAChE conjugates with oxime antidotes can restore the function of the inhibited enzyme. The efficiency of the reactivation reaction depends on several factors, notably the chemical structures of OPs and reactivators and the topography of the AChE active center.[8]

Following phosphylation, a time-dependent elimination reaction occurs on the OP−ChE conjugate that leads to a so-called "aged" enzyme. This reaction can proceed either via dealkylation or deamidation of the phosphorus conjugate, depending on the OP structure.[9−12] The aging reaction results in a very stable anionic conjugate that is resistant to oxime reactivation. Crystal structures of aged phosphyl−AChE conjugates have been produced for *Torpedo califonica* and mouse enzymes inhibited by soman, sarin, tabun, VX, fenamiphos, and diisopropyl fluorophosphate (DFP).[13−19]

Inhibition of hAChE by tabun and the subsequent aging reaction are of particular interest; the conjugate indeed displays an extraordinary resistance toward most oxime reactivators.[20] On the basis of a mass spectrometry (MS) analysis of aged products of tabun-inhibited hAChE, it was suggested that the aging mechanism of tabun−AChE conjugate involved deamination of the phosphoramidate moiety.[4,21] A first crystallographic study on mouse AChE (mAChE) seemed to support a deamination-based aging mechanism,

†The atomic coordinates and structure factors (code 2X8B) have been deposited in the RCSB Protein Data Bank (www.rcsb.org).

*To whom correspondence should be addressed. Tel: +33476639765. Fax: +33476636962. E-mail: florian@nachon.net.

[a]Abbreviations: ACh, acetylcholine; AChE, acetylcholinesterase; BChE, butyrylcholinesterase; ChE, cholinesterase; CHO, Chinese hamster ovary; FAS-II, fasciculin-II; HEPES, *N*-2-hydroxyethylpiperazine-*N*-2-ethanesulfonic acid; hAChE, human AChE; mAChE, mouse AChE; OP, organophosphate; PAS, peripheral anionic site; *Tc*AChE, *Torpedo californica* AChE; T_m, melting temperature.

 Published on Web 04/21/2010

but incomplete aging blurred the interpretation.[22] However, a recent MS study of tabun-inhibited human BChE (hBChE) peptide fragments showed that the loss of the dimethylamine substituent is rather an acid-catalyzed hydrolysis, which occurs during preparation of MS samples,[16] leading to uncertainties on the tabun aging mechanism.

Crystallographic studies on hBChE inhibited by tabun and reinterpretation of mAChE data were at the time undertaken and evidenced that aging of these ChEs proceeds through dealkylation of the ethoxy group.[16] According to the proposed mechanism, the His447 imidazolium stabilizes a developing negative charge on the C−$O^{\delta-}$ oxygen of the ethoxy substituent of the tabun−ChE conjugate, thus polarizing and weakening the C−O bond. Then, a water molecule, stabilized by Glu202, assists the bond breakage by trapping the short-lived developing carbocationic center on the $C^{\delta+}$−O carbon (Scheme 1). This role of water during the dealkylation of an ethoxy substituent was originally suggested by a crystallographic study of hBChE inhibited by echothiophate.[23] However, aging of the tabun−mAChE conjugate was incomplete in the earlier crystallographic studies, complicating the interpretation of the electron density maps. A crystal structure of fully aged tabun-inhibited AChE was needed, especially that of hAChE.

Crystallization of hAChE requires that it is complexed with fasciculin-II (FAS-II), a three-fingered toxin.[24] FAS-II binds tightly to AChE PAS[1] and promotes crystal contacts.[25] The hAChE/FAS complex is reminiscent of the complexes form by FAS with mAChE[26] and *T. californica* AChE (*Tc*AChE).[27] The main feature of the complexes is a sulfur−π interaction between Met33 from FAS-II and Trp286 (Trp279 in *Tc*AChE) at the rim of the active site gorge (Figure 1). The toxin completely caps the gorge entrance (interacting surface: 1045 Å^2), thereby preventing access to the active site. The interaction surface involves all conserved structural elements that constitute the gorge, viz. the Ω loop (C69−C96), the PAS, the acyl loop (W286−S298), and helix 334−341.

To conclude on the aging pathway of tabun-inhibited hAChE, we undertook its crystal structure determination following formation of the aged conjugate in solution. Effects of FAS-II and tabun aging on hAChE thermal denaturation were also investigated and drew insights into the stabilization mechanism in hAChE; our results indicate that the interaction of the two subdomains that face one another across the active site gorge is the main contributor to AChE resilience.

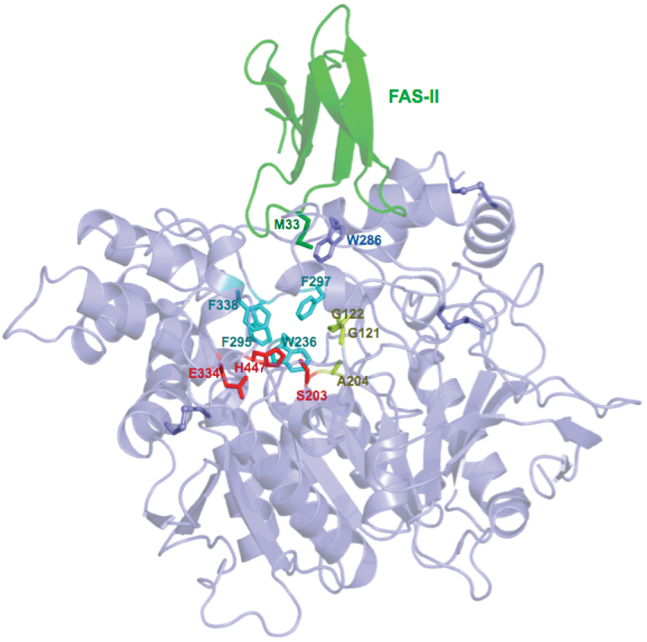

Figure 1. Overview of hAChE/FAS-II complex. hAChE (blue) and fasciculin (green) are represented by cartoons. Key residues are represented as sticks with the catalytic triad in red, the acyl-binding pocket in cyan, and the oxyanion hole in yellow.

Materials and Methods

Racemic tabun solution (2 mg/mL) in isopropanol was from CEB (Vert-le-Petit, France). FAS-II from *Bungarus* venom was purchased from Latoxan (Valence, France). Tabun is a highly toxic chemical warfare agent that belongs to schedule 1 Chemicals (Chemical Weapons Convention). All works with tabun are regulated by the convention. Handling of tabun is dangerous and requires trained personal protection and secured facilities.

Production of Recombinant hAChE. The full cDNA of hAChE was inserted into pGS vector carrying the Glutamine Synthetase gene marker and expressed in Chinese hamster ovary (CHO)-K1 cells. The cells were maintained in serum-free Ultraculture Medium (BioWhittaker) and transfected using DNA−calcium phosphate coprecipitation. Transfected clones were selected by incubation in media containing methionine sulfoximide. The enzyme, secreted into the culture medium, was purified by affinity chromatography and ion-exchange chromatography as described previously.[16] The enzyme was concentrated to 15 mg/mL using a Centricon-30 ultrafiltration microconcentrator (30000 MW cutoff, from Amicon). The enzyme concentration was determined from its absorbance at 280 nm using a molar extinction coefficient of 1.7 for 1 mg/mL of protein.[28]

Melting Temperature (T_m) Determination. The fluorescent dye "Sypro-orange" is sensitive to the polarity of its environment and thus can be used to monitor protein unfolding. Unfolding results in exposure of protein hydrophobic regions, to which the dye binds; this leads to a large increase in fluorescence intensity of dye upon binding.[29] Each hAChE complex (free hAChE, aged tabun−hAChE, hAChE/FAS-II, and aged tabun−hAChE/FAS-II) was diluted to a final concentration of 5 μM in a solution containing 20 mM *N*-2-hydroxyethylpiperazine-*N*-2-ethanesulfonic acid (HEPES), pH 7.5, 0.15 M NaCl, and 0.15 mM Sypro Orange (Molecular Probes). Samples were brought from 25 to 95 °C at a heating rate of 1 °C/min in a real-time PCR machine (Stratagene Mx3005P; accuracy, ±0.25 °C).

Scheme 1. Tabun Inhibition Mechanism on ChEs and Subsequent Aging Mechanism

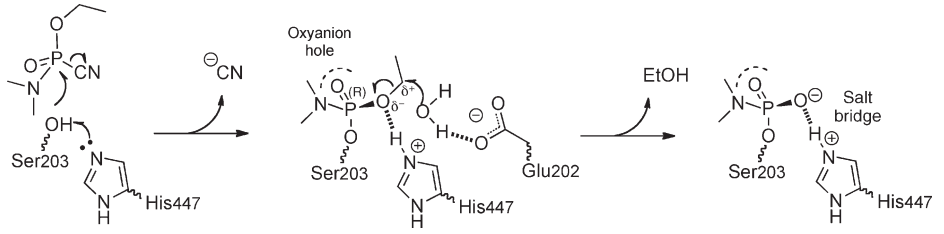

Protein unfolding was monitored through the increase in fluorescence of the Sypro Orange probe and was recorded every minute using the Sybr-Green parameters (wavelength excitation/emission: 492/516 nm). The fluorescence intensity change rate (dF/dT) was plotted as a function of temperature and then normalized. The T_m, corresponding to the temperature at the inflection point, that is, the midtransition of unfolding, was estimated through a nonlinear fit.

Crystallization of Aged Tabun−hAChE Conjugate Complexed with FAS-II. Purified hAChE (0.1 mM) was inhibited in solution, in the presence of 1 mM tabun in 10 mM HEPES buffer, pH 7.4. The reaction mixture was incubated for 1 h at 4 °C. The inhibited enzyme was then combined with FAS-II (0.2 mM) in 10 mM HEPES buffer, pH 7.4, as described.[25] The ternary complex was crystallized at a concentration of 0.1 mM, using the hanging drop method. The mother liquor solution was 0.1 M HEPES buffer, pH 7.4, and 1.3 M ammonium sulfate. An equal amount of the protein and the mother liquor were mixed to yield a 3 μL drop. Crystals grew within a week at 10 °C. The crystals were transferred to a cryoprotecting solution (0.1 M HEPES buffer, pH 7.4, 1.6 M ammonium sulfate, and 18% glycerol) for few seconds before they were flash cooled in liquid nitrogen. The time span between tabun phosphylation of hAChE and flash cooling was > 2 weeks and thus was sufficient for completion of the aging reaction.

X-ray Data Collection, Structure Determination, and Refinement of Tabun−hAChE/FAS-II Conjugate. Diffraction data were collected at the European Synchrotron Radiation Facility (ESRF, Grenoble) on beamline ID14-eh1, at a wavelength of 0.933 Å. Data sets were processed with XDS.[30] The structure was solved by molecular replacement with Phaser,[31] using a starting model of the structure of recombinant hAChE in complex with FAS-II (PDB code: 1B41) without ligands, carbohydrates, and waters. The model was refined using REFMAC5[32] and PHENIX.[33] Iterative cycles of model building were performed with Coot.[34] Ligand descriptions were generated by the PRODRG2.5 server (http://davapc1.bioch.dundee.ac.uk/prodrg/).[35] TLS refinement was performed and yielded significant decreases in R_{cryst} and R_{free} values. TLS groups were defined using the TLSMD server (http://skuld.bmsc.washington.edu/~tlsmd/index.html).[36] A SA composite omit map was calculated, allowing to decrease bias from the model. Protein structures were illustrated using the program PyMOL (http://www.pymol.org).[37]

Results and Discussion

Aged Tabun−hAChE Structure and Inferred Aging Mechanisms. hAChE was inhibited and aged in solution, thus avoiding any possible bias that could arise from inhibition and aging in crystallo. Cocrystals of the aged tabun−hAChE/FAS-II complex diffracted to 2.95 Å. Data and refinement statistics are shown in Table 1. The structure is globally similar to the native hAChE/FAS-II complex (PDB code: 1B41; rmsd = 0.3 Å). Despite expression of the full-length enzyme, residues after 543 are not defined in the electron density maps. Surface loop residues 259−264 are not visible, but external loop residues 493−494, which were not seen in the original structure (PDB code: 1B41), could be modeled.

In the experimental $|F_o| - |F_c|$ map, a strong positive peak is observed (11.7σ) at covalent bonding distance of the catalytic Ser203 hydroxyl oxygen (distance, 1.6 Å), a signature for the phosphorus atom of the tabun adduct. The structure was unambiguously refined as a *N*,*N*-dimethylphosphoramidyl adduct, indicating that the aged adduct results from the dealkylation of tabun P(R) enantiomer (Figure 2). This is faithfully in agreement with the aging mechanism described for tabun-inhibited hBChE and mAChE.[16] The dimethylamino substituent is located in the acyl-binding pocket, with its methyl groups interacting with Trp236 and Phe338 aromatic rings (closest distance between carbon atoms, 3.5 Å to Trp236CZ and Phe338CZ). The oxygen O2 of the phosphoramidate moiety is H-bonded to the main chain nitrogens of the three constituents of the oxyanion hole, viz. Gly121 (2.5 Å), Gly122 (2.7 Å), and Ala204 (3.0 Å). Another strong positive peak is observed in the initial $|F_o| - |F_c|$ map, in the vicinity of Trp86 (5.4σ). We were not able to correctly model this density, but the electron-rich microenvironment provided by the phosphoramidate oxyanion O3, Glu202, and the π-system of Trp86 suggests that it is a positively charged molecule, eventually a weakly coordinated cation. X-ray fluorescence spectra indicate the presence of zinc in the crystals, eventually coming from the plasticware used in the crystallization setup. However, an anomalous map did not confirm the of presence zinc in the active site.

It was already shown that hAChE reacts preferably with one enantiomer of tabun,[16] in accordance with earlier measurements showing that (−)-tabun reacts 6.3 times faster than (+)-tabun with electric eel AChE.[38] However, the absolute configuration of (−)-tabun is unknown. Although the absolute configuration of the nonaged hAChE conjugate can be predicted from the crystal structure, we cannot ascertain which of the two enantiomers is preferred without making assumptions as per the inhibition mechanism. It is

Table 1. Data Collection and Refinement Statistics

data	aged tabun−hAChE/FAS-II PDB code: 2X8B
space group	*H*32
unit cell axes, *a*, *b*, *c* (Å)	151.31, 247.24
no. of measured reflections	206989
unique reflections	22948
resolution (Å)	46.3−2.95 (3.0−2.95)
completeness (%)	98.2 (98.8)
*R*sym (%)[a]	8.2 (66.7)
$I/\acute{o}(I)$	25.0 (3.5)
redundancy	7.2 (7.0)
refinement statistics	
R-factor[b] (*R*-free[c])	18.3 (25.3)
no. of atoms	
protein	4 655
water	235
ligands	47
Wilson *B*-factor (Å^2)	61.3
average *B*-factor (Å^2)	
protein	59.5
water	105.4
ligands	72.7
Ramachandran statistics (%)	
core	84.2
allowed regions	14.1
generously allowed region	0.8
disallowed regions	0.8
rms from ideality	
bond length (Å)	0.006
angles (deg)	0.999
chiral (Å^3)	0.066

[a] $R_{sym} = (\Sigma|I - \langle I\rangle|)/\Sigma I$, where I is the observed intensity and $\langle I\rangle$ is the average intensity obtained from multiple observations of symmetry-related reflections after rejections. [b] *R* factor $= \Sigma||F_o| - |F_c||/\Sigma|F_o|$, where F_o and F_c are observed and calculated structure factors. [c] *R*-free set uses 5% of randomly chosen reflections.

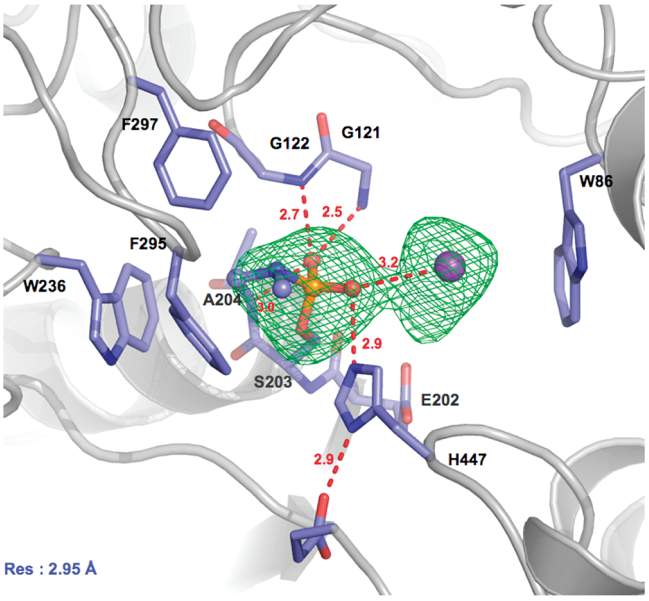

Figure 2. Active site of aged tabun−hAChE/FAS-II conjugate. Key residues are represented as sticks with carbon atoms in blue, nitrogen atoms in deep blue, the phosphorus atom in orange, and oxygen atoms in red. Hydrogen bonds are represented by red dashes. The electron density $|F_o| - |F_c|$ omit map is represented by green mesh contoured at 3σ. The blob of electron density between Trp86 and the phosphyl moiety was interpreted as a disordered cation interacting with the π-system of Trp86, the phosphyl oxyanion, and the negatively charged Glu202 residue.

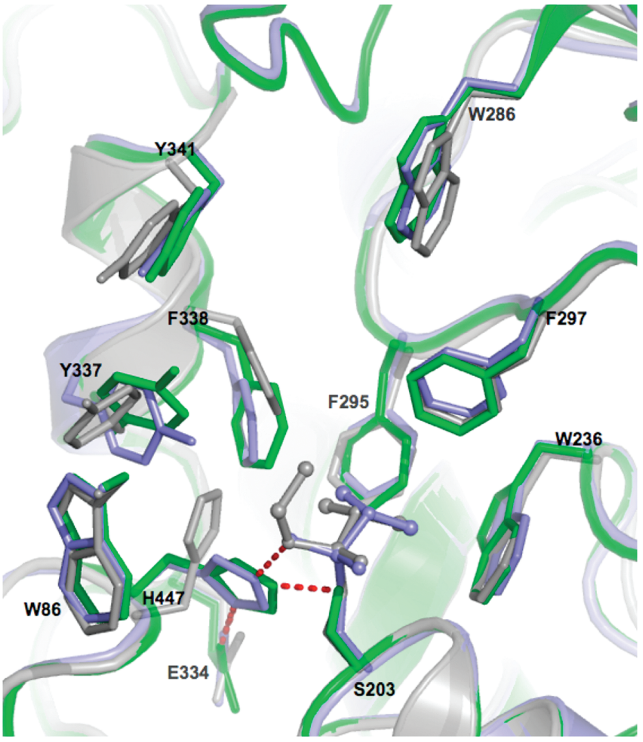

Figure 3. Superimposition of X-ray structures of hAChE/FAS-II in green (1B41), nonaged tabun−mAChE in gray (3DL4), and aged tabun−hAChE/FAS-II in blue (2X8B).

usually assumed that phosphylation occurs "in-line", that is, with the leaving group (CN) oriented opposite to the catalytic serine.[39] According to this mechanism, (*R*)-tabun reacts with hAChE to form the observed P(R) ethyl *N*,*N*-dimethylphosphoramidyl adduct. However, a recent QM/MM study reported that the "in-line" reaction is energetically less favorable than that which would occur if the departing group were adjacent to the catalytic serine.[40] In this proposed mechanism, (*S*)-tabun enatiomer should react with hAChE to form the observed P(R) ethyl *N*,*N*-dimethylphosphoramidyl adduct. This hypothesis is supported by the phosphylation mechanism of optically active dioxaphosphadecalins.[41] Its confirmation will require determination of the absolute configuration of (±)-tabun and crystallographic studies of hAChE inhibited by the pure tabun enantiomers.

Comparison of Free- and Tabun-Inhibited hAChE/FAS-II Complexes. The structures of hAChE/FAS-II and aged tabun−hAChE/FAS-II are very similar. Only limited conformational changes occurs upon aging of the enzyme (Figure 3). A slight tilt of His447 is observed (changes in $\chi1$ and $\chi2$ are 15° for both), resulting from the formation of a salt bridge between phosphoramidate O3 and His447Nε2. The most important conformational change concerns Tyr337, whose Cα shifts by 0.9 Å, while its side chain adopts a new rotamer (changes in $\chi1$ and $\chi2$ are +70 and −27°, respectively). The conformation of Tyr337 in the aged tabun−hAChE/FAS-II structure results in interaction between the Tyr337OH and the cation bound in the choline-binding pocket. This conformer of Tyr337 is further stabilized by a parallel aromatic stacking with Phe338, whose side chain $\chi2$ angle also changes by +40°. This conformation is actually very close to that observed in mAChE−FAS-II complex[42] (PDB code: 1KU6). By contrast, both aromatics are involved in a T-stacking interaction in the hAChE−FAS-II complex. Still, Tyr337 orientation in hAChE−FAS-II is likely influenced by the presence of a ligand visible in the electron density map, modeled as a tight group of three water molecules.[25] We note that Tyr337 in hAChE is equivalent to Phe330 in *Tc*AChE; this residue was also shown to rotate toward the active site upon binding of substrate and substrate reaction product, thereby acting as a bouncer that prevents access to the active site when it is already occupied.[43]

Conformational Changes upon Aging. Recently, we reported the structures of nonaged and aged forms of tabun conjugate with mAChE.[16] The fact that aging was incomplete in mAChE made impossible the characterization of conformational changes that occur upon aging. Here, we report the structure of a completely aged conjugate of tabun with hAChE. Because FAS is required for hAChE to crystallize, it was not possible to obtain the nonaged tabun−hAChE structure. Therefore, we are left with no better option than to critically compare the nonaged tabun−mAChE and aged tabun−hAChE structures. This interspecies structural comparison is yet likely of relevance, since all key residues in the active site gorge, apart from Tyr337 (discussed earlier), are identical and adopt the same conformation in mAChE and hAChE (rmsd < 0.5 Å). Thus, it is expected that conformational differences between the nonaged tabun−mAChE and the aged tabun−hAChE structures mostly reflect the rearrangement of residues upon aging.

Changes resulting from aging of tabun−hAChE are not limited to catalytic histidine movement as seen for the aged VX−*Tc*AChE conjugate;[13] rather, they extend to residues in helix 334−341, one constituent of the active site gorge wall. The large concerted movement of helix 334−341 originates from the release of steric strain upon dealkylation of bound tabun. In the nonaged conjugate structure, the side chain of

catalytic His447 is pushed away from its native position ($\chi1 = 178°$, and $\chi2 = 80°$) by the ethoxy substituent of tabun ($\chi1 = 48°$, and $\chi2 = 61°$). Upon aging, it is allowed to switch back to its original conformation and to reform a strong hydrogen bond with its catalytic triad partner, Glu334, on top of the above-mentioned salt bridge with phosphoramidate O3. Noteworthy is the 3 Å shift of the Phe338 aromatic ring that allows it to maintain contact with the side chain of His447, while stacking against that of Phe295. Together with the reorientation of Tyr337, this leads to the formation of an aromatic stacking pile made of Tyr337, Phe338, and Phe295.

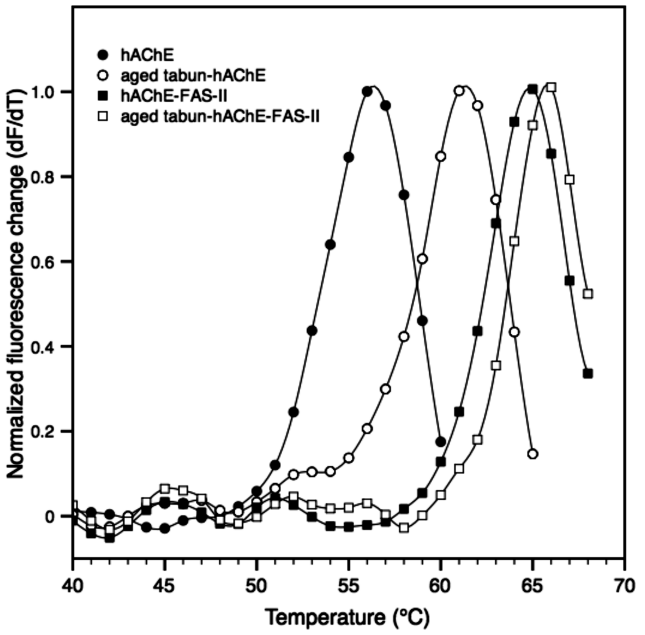

Figure 4. Thermostability of hAChE and its complexes with tabun and FAS-II was determined by a fluoresence-based thermal shift assay. Normalized plots of fluorescence change as a function of temperature were represented for hAChE (●), aged tabun−hAChE (○), hAChE/FAS-II (■), and aged tabun−hAChE/FAS-II (□). The T_m determined at the maximum of fluorescence change was about 56.1, 61.1, 64.8, and 65.8 °C, respectively.

An important question is whether dealkylation precedes His447 reorientation or vice versa. Data gathered so far on the role of His447 (or its equivalent) in the aging of ChEs boils down to the following: (i) Catalytic His447 (or its equivalent) is mobile in AChEs[13,44−46] and immobile in hBChE.[16,23] (ii) The absence of mobility of hBChE's catalytic His438 arises from stabilization by adjacent aromatic residue Phe398: Phe398 restricts the conformational freedom of His438 and stabilizes its protonated form by a π-charge interaction. hAChE lacks this stabilizing effect as Phe398 is replaced by aliphatic residue Val407.[45] (iii) The locked hBChE's histidine is in a conformation always favorable for water-assisted dealkylation of OP ethoxy-substituted adducts by contrast to the mobile histidine of AChEs, which explains why BChEs generally age faster than AChEs.[11,23,47] Altogether, these data suggest that the catalytic His447 should be in its native position to promote tabun dealkylation. It is likely, however, that the steric strain imposed by the presence of the adduct disfavors this conformation in hAChE, thereby delaying aging. Accordingly, any mutation stabilizing the non-native conformation of His447 should slow down the aging process. We believe that this explains the 160-fold decrease in soman−hAChE aging rate for the F338A mutation.[48] Indeed, the mutation leads to the apparition of a void in between Tyr337 and Phe295, where it is possible that the His447 side chain may fit in a conformation unfavorable to aging, similar to that observed in the nonaged tabun−mAChE. Such slow-aging mutants of AChE are of particular interest as pseudo catalytic bioscavengers.[49,50]

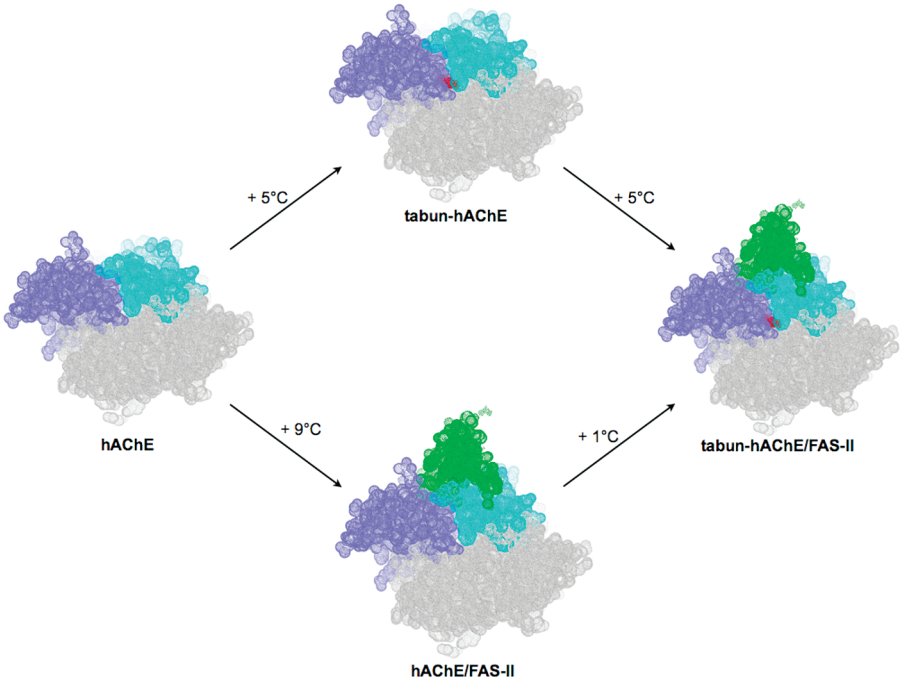

Figure 5. Structural representation of the stabilizing effect of tabun (in red) and fasciculin (in green) on both hAChE subdomains that face one another across the active site gorge. Residues of hAChE are represented by dots and colored in cyan for the first helical subdomain containing the acyl loop and three-helix bundle (241−288) and in blue for the helical second subdomain containing the Ω loop and residues (334−409 and 526−544). The rigid core of hAChE is colored in gray.

Thermostability Screening of hAChE Complexes. Thermostability of cholinesterases (ChEs) has been shown to increase in the presence of bound ligands or upon aging.[51,52] To estimate the relative contributions of FAS-II and aging on the stability of hAChE, we determined the midpoint denaturation temperature (T_m) of native hAChE, aged tabun−hAChE, hAChE/FAS-II, and aged tabun−hAChE/FAS-II. The T_m, corresponding to the temperature where $dF/dt = 0$, that is, at mid-denaturation, are 56.1, 61.1, 64.8, and 65.8 °C for native hAChE, aged tabun−hAChE, hAChE/FAS-II, and aged tabun−hAChE/FAS-II, respectively (Figure 4). There is a significant increase in T_m of hAChE inhibited by aged tabun as compared to native hAChE (+5 °C) and a much larger one for hAChE complexed with FAS-II (+9 °C). This indicates that the stabilizing effect arising from the complexation of FAS-II with hAChE is stronger than that coming from the aged adduct. In view of the hAChE/FAS-II structure, this is faithfully understandable; while the aged adduct stabilizes the enzyme by interactions mostly confined in the active site and the bottom part of the acyl loop, interaction with FAS tightly associates the two subdomains that face one another across the active site gorge, the acyl loop, and the Ω loop (Figure 5). There is a marginal increase in the T_m of aged tabun−hAChE/FAS-II ternary complex as compared to that of hAChE/FAS-II (+1 °C), indicating no significant additional contribution of the aged adduct to the stabilization provided by fasciculin (Figure 5).

In summary, we report the first structure of human AChE inhibited by a nerve agent. This structure provides structural insight on the inhibition and aging mechanisms and infers that tabun aging proceeds via dealkylation of the ethoxy substituent. It also provides a structural template to design new molecules for reactivating aged hAChE.

Acknowledgment. We gratefully acknowledge the ESRF for beam time under long-term projects MX498 and MX722 (IBS BAG) and the ESRF staff for providing efficient help during data collection. Financial support by the Agence Nationale de la Recherche (ANR) under project ANR-06-BLAN-0163, DTRA under contract CBDIF07-THER01-2-0038, and Direction Générale pour l'Armement (DGA) Grants PEA/08co501 and DGA-REI 2009-34-0023.

Supporting Information Available: Morphing movie between nonaged tabun-inhibited mouse AChE and aged tabun-inhibited human AChE structure. This material is available free of charge via the Internet at http://pubs.acs.org.

References

(1) Karlsson, E.; Mbugua, P. M.; Rodriguez-Ithurralde, D. Fasciculins, anticholinesterase toxins from the venom of the green mamba Dendroaspis angusticeps. *J. Physiol.* (*Paris*) **1984**, *79*, 232–240.
(2) Greenblatt, H. M.; Dvir, H.; Silman, I.; Sussman, J. L. Acetylcholinesterase: A multifaceted target for structure-based drug design of anticholinesterase agents for the treatment of Alzheimer's disease. *J. Mol. Neurosci.* **2003**, *20*, 369–383.
(3) Moretto, A. Experimental and clinical toxicology of anticholinesterase agents. *Toxicol. Lett.* **1998**, *102−103*, 509–513.
(4) Barak, D.; Ordentlich, A.; Kaplan, D.; Barak, R.; Mizrahi, D.; Kronman, C.; Segall, Y.; Velan, B.; Shafferman, A. Evidence for P-N bond scission in phosphoroamidate nerve agent adducts of human acetylcholinesterase. *Biochemistry* **2000**, *39*, 1156–1161.
(5) Eddleston, M.; Mohamed, F.; Davies, J. O.; Eyer, P.; Worek, F.; Sheriff, M. H.; Buckley, N. A. Respiratory failure in acute organophosphorus pesticide self-poisoning. *QJM* **2006**, *99*, 513–522.
(6) Konradsen, F. Acute pesticide poisoning—A global public health problem. *Danish Med. Bull.* **2007**, *54*, 58–59.
(7) Sussman, J. L.; Harel, M.; Frolow, F.; Oefner, C.; Goldman, A.; Toker, L.; Silman, I. Atomic structure of acetylcholinesterase from Torpedo californica: a prototypic acetylcholine-binding. *Protein Sci.* **1991**, *253*, 872–879.
(8) Worek, F.; Thiermann, H.; Szinicz, L.; Eyer, P. Kinetic analysis of interactions between human acetylcholinesterase, structurally different organophosphorus compounds and oximes. *Biochem. Pharmacol.* **2004**, *68*, 2237–2248.
(9) Michel, H. O.; Hackley, B. E., Jr.; Berkowitz, L.; List, G.; Hackley, E. B.; Gillilan, W.; Pankau, M. Ageing and dealkylation of Soman (pinacolylmethylphosphonofluoridate)-inactivated eel cholinesterase. *Arch. Biochem. Biophys.* **1967**, *121*, 29–34.
(10) Benschop, H. P.; Keijer, J. H. On the mechanism of ageing of phosphonylated cholinesterases. *Biochim. Biophys. Acta* **1966**, *128*, 586–588.
(11) Li, H.; Schopfer, L. M.; Nachon, F.; Froment, M. T.; Masson, P.; Lockridge, O. Aging pathways for organophosphate-inhibited human butyrylcholinesterase, including novel pathways for isomalathion, resolved by mass spectrometry. *Toxicol. Sci.* **2007**, *100*, 136–145.
(12) Carletti, E.; Aurbek, N.; Gillon, E.; Loiodice, M.; Nicolet, Y.; Fontecilla-Camps, J. C.; Masson, P.; Thiermann, H.; Nachon, F.; Worek, F. Structure-activity analysis of aging and reactivation of human butyrylcholinesterase inhibited by analogues of tabun. *Biochem. J.* **2009**, *421*, 97–106.
(13) Millard, C. B.; Kryger, G.; Ordentlich, A.; Greenblatt, H. M.; Harel, M.; Raves, M. L.; Segall, Y.; Barak, D.; Shafferman, A.; Silman, I.; Sussman, J. L. Crystal structures of aged phosphonylated acetylcholinesterase: Nerve agent reaction products at the atomic level. *Biochemistry* **1999**, *38*, 7032–7039.
(14) Millard, C. B.; Koellner, G.; Ordentlich, A.; Shafferman, A.; Silman, I.; Sussman, J. L. Reaction Products of Acetylcholinesterase and VX Reveal a Mobile Histidine in the Catalytic Triad. *J. Am. Chem. Soc.* **1999**, *121*, 9983–9984.
(15) Hornberg, A.; Tunemalm, A. K.; Ekstrom, F. Crystal structures of acetylcholinesterase in complex with organophosphorus compounds suggest that the acyl pocket modulates the aging reaction by precluding the formation of the trigonal bipyramidal transition state. *Biochemistry* **2007**, *46*, 4815–4825.
(16) Carletti, E.; Li, H.; Li, B.; Ekstrom, F.; Nicolet, Y.; Loiodice, M.; Gillon, E.; Froment, M. T.; Lockridge, O.; Schopfer, L. M.; Masson, P.; Nachon, F. Aging of cholinesterases phosphylated by tabun proceeds through O-dealkylation. *J. Am. Chem. Soc.* **2008**, *130*, 16011–16020.
(17) Sanson, B.; Nachon, F.; Colletier, J. P.; Froment, M. T.; Toker, L.; Greenblatt, H. M.; Sussman, J. L.; Ashani, Y.; Masson, P.; Silman, I.; Weik, M. Crystallographic snapshots of nonaged and aged conjugates of soman with acetylcholinesterase, and of a ternary complex of the aged conjugate with pralidoxime (dagger). *J. Med. Chem.* **2009**, *52*, 7593–7603.
(18) Ekstrom, F.; Hornberg, A.; Artursson, E.; Hammarstrom, L. G.; Schneider, G.; Pang, Y. P. Structure of HI-6*sarin-acetylcholinesterase determined by X-ray crystallography and molecular dynamics simulation: Reactivator mechanism and design. *PLoS One* **2009**, *4*, e5957.
(19) Ekstrom, F. J.; Astot, C.; Pang, Y. P. Novel nerve-agent antidote design based on crystallographic and mass spectrometric analyses of tabun-conjugated acetylcholinesterase in complex with antidotes. *Clin. Pharmacol. Ther.* **2007**, *82*, 282–293.
(20) Worek, F.; Aurbek, N.; Koller, M.; Becker, C.; Eyer, P.; Thiermann, H. Kinetic analysis of reactivation and aging of human acetylcholinesterase inhibited by different phosphoramidates. *Biochem. Pharmacol.* **2007**, *73*, 1807–1817.
(21) Elhanany, E.; Ordentlich, A.; Dgany, O.; Kaplan, D.; Segall, Y.; Barak, R.; Velan, B.; Shafferman, A. Resolving pathways of interaction of covalent inhibitors with the active site of acetylcholinesterases: MALDI-TOF/MS analysis of various nerve agent phosphyl adducts. *Chem. Res. Toxicol.* **2001**, *14*, 912–918.
(22) Ekstrom, F.; Akfur, C.; Tunemalm, A. K.; Lundberg, S. Structural changes of phenylalanine 338 and histidine 447 revealed by the crystal structures of tabun-inhibited murine acetylcholinesterase. *Biochemistry* **2006**, *45*, 74–81.
(23) Nachon, F.; Asojo, O. A.; Borgstahl, G. E.; Masson, P.; Lockridge, O. Role of water in aging of human butyrylcholinesterase inhibited by echothiophate: the crystal structure suggests two alternative mechanisms of aging. *Biochemistry* **2005**, *44*, 1154–1162.
(24) le Du, M. H.; Housset, D.; Marchot, P.; Bougis, P. E.; Navaza, J.; Fontecilla-Camps, J. C. Structure of fasciculin 2 from green mamba snake venom: evidence for unusual loop flexibility. *Acta Crystallogr., Sect. D: Biol. Crystallogr.* **1996**, *52*, 87–92.
(25) Kryger, G.; Harel, M.; Giles, K.; Toker, L.; Velan, B.; Lazar, A.; Kronman, C.; Barak, D.; Ariel, N.; Shafferman, A.; Silman, I.;

Sussman, J. L. Structures of recombinant native and E202Q mutant human acetylcholinesterase complexed with the snake-venom toxin fasciculin-II. *Acta Crystallogr., Sect. D: Biol. Crystallogr.* **2000**, *56*, 1385–1394.
(26) Bourne, Y.; Taylor, P.; Marchot, P. Acetylcholinesterase inhibition by fasciculin: crystal structure of the complex. *Cell* **1995**, *83*, 503–512.
(27) Harel, M.; Kleywegt, G. J.; Ravelli, R. B.; Silman, I.; Sussman, J. L. Crystal structure of an acetylcholinesterase-fasciculin complex: interaction of a three-fingered toxin from snake venom with its target. *Structure* **1995**, *3*, 1355–1366.
(28) Rosenberry, T. L.; Scoggin, D. M. Structure of human erythrocyte acetylcholinesterase. Characterization of intersubunit disulfide bonding and detergent interaction. *J. Biol. Chem.* **1984**, *259*, 5643–5652.
(29) Lo, M. C.; Aulabaugh, A.; Jin, G.; Cowling, R.; Bard, J.; Malamas, M.; Ellestad, G. Evaluation of fluorescence-based thermal shift assays for hit identification in drug discovery. *Anal. Biochem.* **2004**, *332*, 153–159.
(30) Kabsch, W. XDS. *Acta Crystallogr., Sect. D: Biol. Crystallogr.* **2010**, *66*, 125–132.
(31) McCoy, A. J.; Grosse-Kunstleve, R. W.; Adams, P. D.; Winn, M. D.; Storoni, L. C.; Read, R. J. Phaser crystallographic software. *J. Appl. Crystallogr.* **2007**, *40*, 658–674.
(32) Murshudov, G. N.; Vagin, A. A.; Dodson, E. J. Refinement of macromolecular structures by the maximum-likelihood method. *Acta Crystallogr., Sect. D: Biol. Crystallogr.* **1997**, *53*, 240–255.
(33) Adams, P. D.; Afonine, P. V.; Bunkoczi, G.; Chen, V. B.; Davis, I. W.; Echols, N.; Headd, J. J.; Hung, L. W.; Kapral, G. J.; Grosse-Kunstleve, R. W.; McCoy, A. J.; Moriarty, N. W.; Oeffner, R.; Read, R. J.; Richardson, D. C.; Richardson, J. S.; Terwilliger, T. C.; Zwart, P. H. PHENIX: A comprehensive Python-based system for macromolecular structure solution. *Acta Crystallogr., Sect. D: Biol. Crystallogr.* **2010**, *66*, 213–221.
(34) Emsley, P.; Cowtan, K. Coot: Model-building tools for molecular graphics. *Acta Crystallogr., Sect. D: Biol. Crystallogr.* **2004**, *60*, 2126–2132.
(35) Schüttelkopf, A. W.; Van Aalten, D. M. F. PRODRG: A tool for high-throughput crystallography of protein-ligand complexes. *Acta Crystallogr., Sect. D: Biol. Crystallogr.* **2004**, *D60*, 1355–1363.
(36) Painter, J.; Merritt, E. A. Optimal description of a protein structure in terms of multiple groups undergoing TLS motion. *Acta Crystallogr., Sect. D: Biol. Crystallogr.* **2006**, *62*, 439–450.
(37) DeLano, W. L. *The PyMol Molecular Graphics System*; DeLano Scientific LLC: San Carlos, CA, 2002.
(38) Degenhardt, C. E.; Van Den Berg, G. R.; De Jong, L. P. A.; Benschop, H. P.; Van Genderen, J.; Van De Meent, D. Enantiospecific complexation gas chromatography of nerve agents. Isolation and properties of the enantiomers of ethyl N,N-dimethylphosphoramidocyanidate (tabun). *J. Am. Chem. Soc.* **1986**, *108*, 8290–8291.
(39) Järv, J. Stereochemical aspects of cholinesterase catalysis. *Bioorg. Chem.* **1984**, *12*, 259–278.
(40) Kwasnieski, O.; Verdier, L.; Malacria, M.; Derat, E. Fixation of the two tabun isomers in acetylcholinesterase: A QM/MM study. *J. Phys. Chem. B* **2009**, *113*, 10001–10007.
(41) Furegati, S.; Zerbe, O.; Ruedi, P. The stereochemistry of the inhibition of acetylcholinesterase with acetylcholine-mimetic 7-aza-2,4-dioxaphosphadecalins. *Chem.-Biol. Interact.* **2005**, *157−158*, 418–420.
(42) Bourne, Y.; Taylor, P.; Radic, Z.; Marchot, P. Structural insights into ligand interactions at the acetylcholinesterase peripheral anionic site. *EMBO J.* **2003**, *22*, 1–12.
(43) Colletier, J. P.; Fournier, D.; Greenblatt, H. M.; Stojan, J.; Sussman, J. L.; Zaccai, G.; Silman, I.; Weik, M. Structural insights into substrate traffic and inhibition in acetylcholinesterase. *EMBO J.* **2006**, *25*, 2746–2756.
(44) Massiah, M. A.; Viragh, C.; Reddy, P. M.; Kovach, I. M.; Johnson, J.; Rosenberry, T. L.; Mildvan, A. S. Short, strong hydrogen bonds at the active site of human acetylcholinesterase: Proton NMR studies. *Biochemistry* **2001**, *40*, 5682–5690.
(45) Kaplan, D.; Barak, D.; Ordentlich, A.; Kronman, C.; Velan, B.; Shafferman, A. Is aromaticity essential for trapping the catalytic histidine 447 in human acetylcholinesterase? *Biochemistry* **2004**, *43*, 3129–3136.
(46) Hornberg, A.; Artursson, E.; Warme, R.; Pang, Y. P.; Ekstrom, F. Crystal structures of oxime-bound fenamiphos-acetylcholinesterases: reactivation involving flipping of the His447 ring to form a reactive Glu334-His447-oxime triad. *Biochem. Pharmacol.* **2010**, *79*, 507–515.
(47) Aldridge, W. N.; Reiner, E. *Enzyme Inhibitors as Substrates*; North-Holland Publishing Co.: Amsterdam, 1972.
(48) Shafferman, A.; Ordentlich, A.; Barak, D.; Stein, D.; Ariel, N.; Velan, B. Aging of phosphylated human acetylcholinesterase: catalytic processes mediated by aromatic and polar residues of the active centre. *Biochem. J.* **1996**, *318* (Part 3), 833–840.
(49) Shafferman, A.; Barak, D.; Stein, D.; Kronman, C.; Velan, B.; Greig, N. H.; Ordentlich, A. Flexibility versus "rigidity" of the functional architecture of AChE active center. *Chem.-Biol. Interact.* **2008**, *175*, 166–172.
(50) Shafferman, A. Next generation of OP-bioscavengers. International Meeting on Cholinesterases, Sibenik, Croatia **2009**, oral communication.
(51) Masson, P.; Clery, C.; Guerra, P.; Redslob, A.; Albaret, C.; Fortier, P. L. Hydration change during the aging of phosphorylated human butyrylcholinesterase: importance of residues aspartate-70 and glutamate-197 in the water network as probed by hydrostatic and osmotic pressures. *Biochem. J.* **1999**, *343* (Part 2), 361–369.
(52) Rochu, D.; Clery-Barraud, C.; Renault, F.; Chevalier, A.; Bon, C.; Masson, P. Capillary electrophoresis versus differential scanning calorimetry for the analysis of free enzyme versus enzyme-ligand complexes: in the search of the ligand-free status of cholinesterases. *Electrophoresis* **2006**, *27*, 442–451.